PHYSICAL REVIEW C VOLUME 23, NUMBER 4 APRIL 1981

Contributions from high-momentum intermediate states to effective nucleon-nucleon interactions

H. M. Sommermann,* H. Müther, K. C. Tam,† T. T. S. Kuo,† and Amand Faessler
Institut für Theoretische Physik, Universität Tübingen, D-7400 Tübingen, Germany
(Received 22 September 1980)

We reexamine the intermediate state convergence problem for the core polarization diagram (G_{3p1h}) in the expansion of an effective shell-model interaction using a modern meson exchange Bonn-Jülich potential in comparison to the phenomenological Reid soft-core interaction. The Bonn-Jülich N-N potential contains a much weaker tensor force as compared with the Reid soft-core interaction. As a consequence its repulsive contributions to G_{3p1h} from high momentum intermediate particle states are much reduced and G_{3p1h} can be calculated in a good approximation with $2\hbar\omega$ particle-hole excitations alone. This opens up the possibility of calculating higher order processes in a reliable and expedient way. We have further determined the spectra of ^{18}O and ^{18}F using the folded diagram perturbation theory to determine the effective interaction. The energy levels are best reproduced by the Bonn-Jülich N-N potential.

[NUCLEAR STRUCTURE ^{18}O, ^{18}F; dependence of effective interaction on N-N tensor force. Convergence of intermediate state summation in core polarization.]

I. INTRODUCTION

Core polarization processes have played a very important role in the development of microscopic effective interactions. The significance of the second-order core polarization diagram (G_{3p1h}) was pointed out in the early works of Bertsch[1] and Kuo and Brown.[2] Its primary function is to provide the necessary long-range quadrupole-quadrupole component (P_2 force) in the empirical effective interaction between valence nucleons.[3] Conventionally, this core polarization diagram was calculated with a restricted sum over the intermediate particle-hole harmonic oscillator states: $\epsilon_p - \epsilon_h = 2\hbar\omega$. It was argued that the primary mechanism for core rearrangement should be the excitation of low-energy phonons of the core by the valence nucleons. Vary, Sauer, and Wong[4] (VSW) questioned the validity of this approximation. They included particle-hole excitations up to $22\hbar\omega$ for $A = 18$ nuclei and found a rather slow rate of convergence, usually referred to as the VSW effect. Similar conclusions have also been reached by Kung, Kuo, and Ratcliff[5] (KKR). Both calculations employed the Reid soft-core (RSC) nucleon-nucleon potential.[6] Using this interaction, the contributions to G_{3p1h} from p-h excitations with energy greater than $2\hbar\omega$ were found to be predominantly repulsive, and thereby they almost counterbalanced the attractive contribution form G_{3p1h} with $2\hbar\omega$. In particular, the diagonal $J = 0$, $T = 1$ sd-shell matrix elements acquired, on the average, 500 keV repulsion from excitations with $\epsilon_p - \epsilon_h > 2\hbar\omega$. As a result, the ground state of ^{18}O now received an attractive shift of only about 350 keV over the bare interactions results. $2\hbar\omega$ excitations in the core polarization diagram calculated from RSC are therefore inadequate. The previous good agreement with experiment[2] could not be reproduced by calculations which took into account the excitations to high lying states. This convergence problem poses a major difficulty in the computation of the effective interaction from realistic nucleon-nucleon potentials. First of all, it is numerically quite difficult to calculate core polarization processes with intermediate particle-hole excitations up to $22\hbar\omega$. This puts severe limitations on the extent of such calculations. Moreover, even after having included all these higher excitations and having obtained converged values of G_{3p1h}, the results do not seem to yield adequate long-range multipole components, whose need has been established in the empirical effective interaction.

The slow rate of convergence in the intermediate-state summation can be traced to the tensor component of the Reid soft-core interaction. While central force components alone lead to rapid convergence, the strong tensor force requires one to carry the summation over intermediate p-h states up to very high excitation energies. The energy denominators provide little assistance for convergence.

In a meson exchange theory of the nucleon-nucleon interaction, the intermediate-range tensor force originates from the exchange of pseudoscalar pions and ρ vector-mesons. The ρ-exchange tensor interaction has the opposite sign as compared with the tensor part of the one-pion exchange potential. It is very important for a number of phenomena that the ρ-exchange tensor potential cuts off the one pion-exchange tensor potential at short distances. This is accomplished

 © 1981 The American Physical Society

by choosing a relatively strong ρ-N coupling, which is in agreement with the analysis of Höhler and Pietarinen.[7] The resulting tensor interaction becomes much weaker than in earlier N-N potentials. Recent theoretical studies of the πNN vertex function[8] and new empirical evidence,[9] in fact, suggest a rather weak tensor force. The Reid soft-core interaction, however, contains a very strong tensor force component, which results in a D-state probability of $P_D \approx 6.4\%$ for the deuteron. At present a much smaller D-state probability, $P_D \approx 4\%$, seems favorable, although usual potential models with such a low D-state probability tend to overbind nuclear matter significantly. This discrepancy can be resolved by considering explicit isobar degrees of freedom in the two-nucleon force. This procedure yields modifications of the effective NN interaction in a nuclear medium due to the presence of other nucleons. The medium range attraction of the NN interaction originating from terms with intermediate isobars is reduced by Pauli and dispersion effects. Many-body corrections of this type play a large role, and even in light nuclei such as ^{16}O these effects are not negligible.[10] The Bonn-Jülich (MDFPΔ2) potential[11] is based on this meson theoretical framework and we have used it to investigate the so-called Vary-Sauer-Wong effect. Our main objective is to determine the influence of the tensor force, which is derived from a modern meson exchange interaction, on the convergence properties of the core polarization diagram. Based on our present knowledge of nucleon-nucleon potentials, are we allowed, in a good approximation, to consider only $2\hbar\omega$ intermediate excitations in the calculation of the core polarization diagram G_{3p1h}? Can we show that there is no Vary-Sauer-Wong effect? Is it possible to restore the much needed P_2 force which was thought to originate from G_{3p1h}? The answer to these questions will be crucial for further nuclear structure calculations.

In Sec. II we will formulate the problem of a converged calculation of the core polarization diagram and discuss our treatment of the intermediate state summation. We will briefly review the construction of the microscopic effective interaction and the evaluation of the folded diagram series, from which we obtain the spectra of ^{18}O and ^{18}F. Some interesting technical details are given in Sec. III, including a brief description of rather new momentum-space techniques. Finally, in Sec. IV, we give the results and discussion of our calculation. We will show in this paper the delicate dependence of the above slow convergence behavior on the N-N potential used in the calculation.

II. FORMULATION

In this section we outline our treatment of the core polarization process in a microscopic calculation of the effective interaction between valence nucleons.

In many body perturbation theory we start from a nuclear Hamiltonian H which is given as the sum of a single particle Hamiltonian H_0 plus the residual interaction H_1.

$$H = H_0 + H_1 , \tag{1a}$$

$$H_0 = T + U , \tag{1b}$$

$$H_1 = V - U . \tag{1c}$$

T and V denote, respectively, the kinetic and potential energy of the many body system. The auxiliary one-body potential U is chosen such as to "minimize" the remaining interaction, which consequently is treated by perturbation theory.

In the treatment of low-lying nuclear states the success of the nuclear shell model indicates that the choice of U as a spherical harmonic oscillator potential is appropriate. With this choice the core polarization diagram [Fig. 1(a) diagram (iv)] may be written[5] as

$$\langle abJT|G_{3p1h}|cdJT\rangle = (1+\delta_{ab})^{-1/2}(1+\delta_{cd})^{-1/2} \sum_{p\text{-}h} \sum_{J_1 J_2 T_1 T_2} (2J_1+1)(2J_2+1)(2T_1+1)(2T_2+1)$$

$$\times \begin{Bmatrix} J_2 & j_p & j_a \\ j_n & J_1 & j_b \\ j_c & j_d & J \end{Bmatrix} \begin{Bmatrix} T_2 & \frac{1}{2} & \frac{1}{2} \\ \frac{1}{2} & T_1 & \frac{1}{2} \\ \frac{1}{2} & \frac{1}{2} & T \end{Bmatrix} \langle hbJ_1T_1|G(\omega_f)|pdJ_1T_1\rangle$$

$$\times \left\langle p\left|\frac{1}{\omega_0 - H_0}\right|p\right\rangle \langle apJ_2T_2|G(\omega_i)|chJ_2T_2\rangle \tag{2a}$$

with

$$\omega_f = \epsilon_c + \epsilon_d + \epsilon_h - \epsilon_a , \tag{2b}$$

$$\omega_i = \epsilon_c + \epsilon_h , \tag{2c}$$

$$\omega_0 = \epsilon_c + \epsilon_d . \tag{2d}$$

For the example of ^{18}O or ^{18}F the model space is composed of single particle orbits from the sd shell for the two valence nucleons. The summation for the particle states p ranges over all harmonic oscillator states above the 0s and 0p shells.

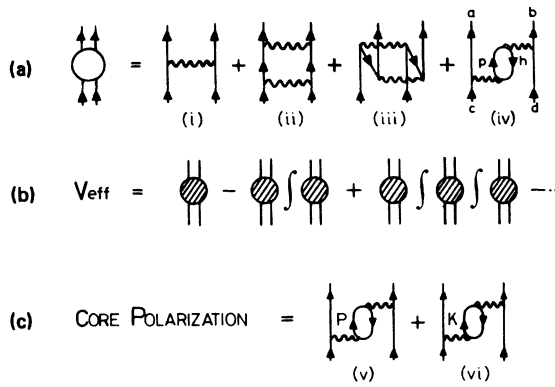

FIG. 1. (a) The particle-particle interaction. The valence particle interaction for $A=18$ nuclei is given up to second order in terms of the Brueckner reaction matrix (denoted by wavy lines). (b) The folded diagram expansion for the effective interaction. The model space effective interaction series is indicated and terms with up to two folds are shown. The cross-hatched box consists of the one-particle Q boxes for each valence nucleon plus the particle-particle interaction of (a). (c) The core polarization process G_{3p1h}. The core polarization diagram has been calculated as the sum of diagrams (v) and (vi). The former contains low-lying intermediate particle states in harmonic oscillator representation while the latter includes the orthogonalized high-lying plane wave particle states.

While low-lying single particle states can be well approximated by harmonic oscillator functions, this clearly does not hold true for highly excited nucleons, and it may be more appropriate to use the choice $U=0$ for these states. The question concerning the choice of the single particle spectrum in the calculation of G_{3p1h} is similar to that in the calculation of the bare Brueckner reaction matrix G,

$$G(\omega)=V+V\frac{Q}{\omega-H_0}G(\omega)\,. \tag{3}$$

Q represents the Pauli exclusion operator. Several authors[12,13] have emphasized the importance of a consistent treatment which leads to the inclusion of $-U$ insertions to all orders in the reaction matrix (remember that $H_1=V-U$). In this section we follow closely the development given by Kung, Kuo, and Ratcliff.[5] The reaction matrix is then defined by

$$G^T(\omega)=V+VQ\frac{1}{\omega-QTQ}QG^T(\omega)\,. \tag{4}$$

The same arguments may be applied to the calculation of the core polarization diagram G_{3p1h}. Adding $-U$ insertions to all orders to the particle line p of G_{3p1h} we are led to a geometric series of the form

$$-\frac{\hat{q}}{\omega_0-H_0}U\frac{\hat{q}}{\omega_0-H_0}+\frac{\hat{q}}{\omega_0-H_0}U\frac{\hat{q}}{\omega_0-H_0}U\frac{\hat{q}}{\omega_0-H_0}-\cdots\,. \tag{5}$$

Together with G_{3p1h} this series can be readily summed up and we obtain

$$\langle ab|G^T_{3p1h}|cd\rangle=\int dk\int dk'\sum_h\langle hb|G|kd\rangle\left\langle k\left|\hat{q}\frac{1}{\omega_0'-\hat{q}t\hat{q}}\hat{q}\right|k'\right\rangle\langle ak'|G|ch\rangle\,. \tag{6}$$

$\hat{q}$ projects onto one-particle oscillator states in the sd shell and above. $\omega_0'=(\epsilon_c+\epsilon_d)-(\epsilon_a+\epsilon_d-\epsilon_h)$. $-U$ insertions to the hole lines in G_{3p1h} will be canceled, essentially, by the corresponding Brueckner-Hartree-Fock (BHF) self-energy insertions, as the BHF self-consistent single particle wave functions for the hole states ($0s_{1/2}$, $0p_{3/2}$, and $0p_{1/2}$) are well represented by harmonic oscillator wave functions. The wave functions of particle states at higher excitation energies should not be expected to resemble harmonic oscillator functions. In fact, for very high excitation energy they should be well represented by free particle states. Thus there exist two different schemes for the evaluation of the core polarization process, denoted by G_{3p1h} and G^T_{3p1h}, respectively. In the first scheme, which corresponds to Eq. (2), no $-U$ insertions are considered. This approach was taken by Vary, Sauer, and Wong. In the second scheme $-U$ insertions are included for the high-lying single particle states. This method leads to Eq. (6) and has been used by Kung, Kuo, and Ratcliff. It may be pointed out that both results are quite similar.[5]

In the present work we will adopt a double partition approach which we regard as most appropriate. We have calculated G^T_{3p1h} for three compound spectra which consist of oscillator states up to $0p$, $1s0d$, and $1p0f$ shells, respectively, and orthogonalized plane waves above these states. This compound spectrum approach corresponds to the exclusion of $-U$ insertions from low-lying states where Brueckner-Hartree-Fock considerations suggest cancellation of such insertions with self-energy bubbles, but inclusion of $-U$ insertions to all orders at energies above which BHF consideration should no longer be applicable.

G^T_{3p1h} represents one term in the expansion of the

effective interaction. After we have studied the convergence problems in G^T_{3p1h}, which arise from the tensor components in the N-N interaction, we would like to evaluate the complete model space effective interaction. We can then determine the theoretical spectra of ^{18}O and ^{18}F and make a comparison with the experimental data. For the calculation of the microscopic effective interaction we employ the folded diagram perturbation theory of Kuo, Lee, and Ratcliff[14] and of Krenciglowa and Kuo.[15] The calculation is carried out in two steps.

We first calculate the Q box as a sum of some irreducible diagrams. Our model space for $A=18$ nuclei consists of two-particle states which are composed of the valence nucleons in the sd shell. The Q box is calculated in low-order perturbation theory up to second order in the reaction matrix [see Fig. 1(a)]. Diagram (i) represents the Brueckner reaction matrix. Diagram (ii) is included to treat the scattering into low-lying two-particle states separate from the excitation of high-lying intermediate two-particle states which are considered in solving the Bethe-Goldstone equation. For that purpose the Bethe-Goldstone equation has been solved using a projection operator P defined in the nomenclature of Ref. 16 by $P(3,10,21)$. Intermediate states in which both particles occupy a sd- or pf-shell orbit, for example, are not considered in the bare reaction matrix (i). Scattering to these states, which are best represented by oscillator wave functions, is treated by calculating diagram (ii). In addition to the core polarization diagram (iv) we also include the process (iii), which we call G_{4p2h}. Please note that there will be no convergence problem for the intermediate state summation except in G_{3p1h}. All other diagrams contain only finite sums over intermediate particles and holes. Diagrams containing bubble insertions have been eliminated since the BHF conditions are reasonably satisfied when using appropriate harmonic oscillator wave functions.

In the second step we evaluate the folded diagram series. Using the derivative method of Kuo, Lee, and Ratcliff[14] we include all terms involving up to four folds. The folded diagram series up to two folds is shown in Fig. 1(b). The Q box in this case is the sum of one-body and two-body irreducible diagrams. After folding, all one-body terms are removed. The complete Hamiltonian is obtained as the sum of a diagonal single particle Hamiltonian containing the empirical single particle energies plus the theoretical model space effective interaction.

III. METHOD OF CALCULATION

A special feature of the present calculation is the evaluation of the reaction matrix elements needed for G^T_{3p1h} in a "mixed representation." They are of the form $\langle n_1 n_2 | G | k_3 n_4 \rangle$, where n_1, n_2, and n_4 are oscillator states and k_3 is a plane-wave state with δ-function normalization. To calculate the G matrix in this mixed representation both Moshinsky brackets and the less known vector brackets are needed. The vector brackets $\langle klKL\lambda | k_3 l_3 k_4 l_4 \lambda \rangle$ facilitate the transformation of two nucleon laboratory frame plane-wave states into relative and center-of-mass coordinates.

$$|k_3 l_3 j_3 k_4 l_4 j_4; JT\rangle = \sum_{\lambda} \sum_{lLS\mathcal{S}} \int dK \int dk \frac{1-(-)^{l+S+T}}{\sqrt{2}} [(2j_3+1)(2j_4+1)(2\lambda+1)(2S+1)]^{1/2} \times \begin{Bmatrix} l_3 & l_4 & \lambda \\ \frac{1}{2} & \frac{1}{2} & S \\ j_3 & j_4 & J \end{Bmatrix} \langle klKL\lambda | k_3 l_3 k_4 l_4 \lambda \rangle [(2\mathcal{S}+1)(2\lambda+1)]^{1/2} W(\mathcal{S}LS\lambda; Jl) | klS(\mathcal{S})KL; JT\rangle . \tag{7}$$

The vector bracket transformation has been extensively discussed by Wong and Clement.[17] The formulation by Balian and Brezin[18] is more convenient for the purpose of numerical calculations. A detailed description of this method in relation to the present problem can be found in Ref. 5.

The reaction matrix is obtained as the sum of the free two-nucleon G matrix G_F minus a Pauli correction term:

$$G(\omega) = V + VQ \frac{1}{\omega - QTQ} QG(\omega) = G_F - \Delta G . \tag{8a}$$

G is calculated according to the method of Krenciglowa, Kung, Kuo, and Osnes[16] using plane wave intermediate states. The Pauli exclusion operator Q is handled with the help of the Tsai-Kuo operator identity[19] which leads to the equations

$$G_F(\omega) = V + V\frac{1}{e}G_F(\omega)\,, \tag{8b}$$

$$\Delta G = G_F\frac{1}{e}P\left[1\Big/P\left(\frac{1}{e}+\frac{1}{e}G_F\frac{1}{e}\right)P\right]P\frac{1}{e}G_F\,. \tag{8c}$$

Similarly, the core polarization diagram G^T_{3p1h} can be expressed as the sum of two terms

$$\langle ab|G^T_{3p1h}|cd\rangle = (\text{free term}) - (\text{Pauli term})\,, \tag{9a}$$

where

$$(\text{free term}) = \sum_h \int dk \langle hb|G|kd\rangle \left\langle k\left|\frac{1}{\omega_0' - t}\right|k\right\rangle \langle ak|G|ch\rangle\,, \tag{9b}$$

$$(\text{Pauli term}) = \sum_h \int dk \int dk' \langle hb|G|kd\rangle \left\langle k\left|\frac{1}{\omega_0' - t}\hat{p}\left[1\Big/\hat{p}\left(\frac{1}{\omega_0' - t}\right)\hat{p}\right]\hat{p}\frac{1}{\omega_0' - t}\right|k'\right\rangle \langle ak'|G|ch\rangle\,. \tag{9c}$$

Here $\hat{p}$ is a one-body operator $\hat{p} = 1 - \hat{q}$ projecting onto the harmonic oscillator single-particle states in the ^{16}O core. ω_0' has been defined in connection with Eq. (6). The core-polarization diagrams, as well as all other graphs, were derived with the help of diagrammatic rules developed by Kuo *et al.*[20]

After we have obtained the Q box as described above, the folded diagram series is obtained using the derivative method of Ref. 14 as previously mentioned. This approach is more suitable in the case of a two valence nucleon system than the iteration scheme of Krenciglowa.[15] We have used a harmonic oscillator shell spacing of $\hbar\omega = 14$ MeV. To test the convergence properties of the folded diagram series, several *sd*-shell single particle energies were employed. This rather interesting point is discussed in detail in Sec. IV.

The calculations are performed using two different *NN* potentials V, the Reid soft core[6] potential and the potential MDFPΔ2 of the Bonn-Jülich group.[11] Both potentials were adjusted to describe the two nucleon data. While, however, the Reid potential to be used in a nuclear many-body calculation is identical to the one which is used in the description of the two nucleon data, this is not the case for the Bonn-Jülich potential. The Bonn-Jülich potential is derived in the framework of meson exchange theory using noncovariant time-dependent perturbation theory. It consists of the terms

$$V = V_{\rm OBE}(\omega) + U_{N\Delta}(\omega)\frac{\tilde{Q}}{\omega - \tilde{H}_0}U_{N\Delta}(\omega) + V_{\Delta\Delta}(\omega)\frac{1}{\omega - \tilde{H}_0}V_{\Delta\Delta}(\omega)\,. \tag{10}$$

The first term of Eq. (10), $V_{\rm OBE}$, is a one boson exchange part of the potential. Due to the treatment within noncovariant perturbation theory, it depends on the starting energy ω. The second and third terms of Eq. (10) describe contributions to the effective *NN* potential where one or both of the interacting nucleons are intermediately excited to the $\Delta(3,3)$ resonance. These terms are graphically represented in Fig. 2. They contribute significantly to the medium range attractive parts of the *NN* potential. While, however, for the two-nucleon system the operator $\tilde{Q}$ in Eq. (10) is set equal to one, for the interaction of two nucleons in a nucleus, the Pauli operator $\tilde{Q}$ prevents intermediate $N\Delta$ states with nucleons in occupied states. This Pauli quenching reduces the attractive second term of Eq. (10) and therefore yields less attractive matrix elements for *NN* states with isospin $T = 1$. Also, the modification of the propagators of Eq. (10), which in a nuclear medium are defined in terms of self-consistent single particle rather than kinetic energies, yields a reduction of the terms with intermediate isobars. This effect is usually referred to as dispersion quenching. A more detailed description of the technical treatment of this effective consideration of mesonic and isobar degrees of freedom of the *NN* interaction is given in Ref. 11.

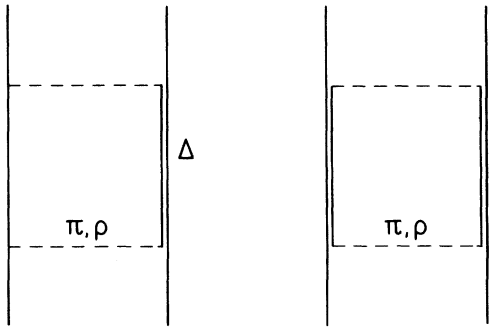

FIG. 2. Graphical representation of contributions to the Bonn-Jülich effective potential due to excitation of intermediate $\Delta(3,3)$ states. The diagrams correspond to the second and third terms of Eq. (10).

IV. RESULTS AND DISCUSSION

We begin the presentation of our results with a discussion of the momentum dependence (k_3) of the reaction matrix $\langle n_1 n_2 | G | k_3 n_4 \rangle$ and its influence on the convergence behavior of G^T_{3p1h}. We then give some numerical results for G^T_{3p1h} calculated from the Bonn-Jülich and Reid soft-core potentials and make a statement about their respective Vary-Sauer-Wong effects. Finally, the complete effective interaction of Figs. 1(a) and 1(b) is calculated and the resulting spectra of ^{18}O and ^{18}F are studied in detail. In this context we also investigate the convergence behavior of the effective interaction expansion.

In Fig. 3 we show two representative G-matrix elements plotted as a function of the intermediate particle momentum k. The matrix element in the lower part contains primarily contributions from the central components of the N-N potential. The Bonn-Jülich (MDFPΔ2) and RSC potentials show a very similar behavior in this case. The reaction matrix element which is displayed in the upper part of Fig. 3 is dominated by the tensor interaction in the N-N interaction. Note the large peak at high particle momenta in the case of the Reid potential. In a harmonic oscillator representation its contributions to G_{3p1h} are only included when summing over particle-hole excitations with energies much larger than $2\hbar\omega$. The same matrix element, calculated from the Bonn-Jülich potential, peaks at the same particle momentum. Its magnitude, however, is drastically reduced when compared with the corresponding RSC matrix element.

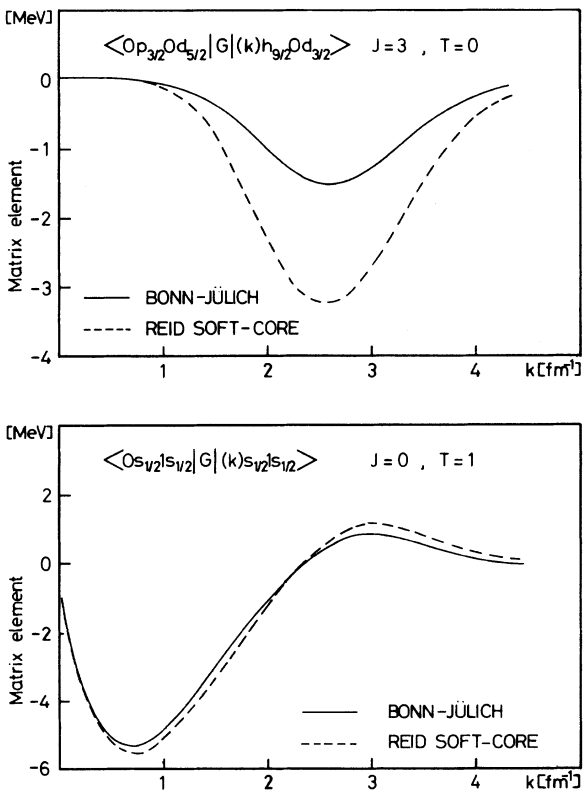

FIG. 3. Reaction matrix elements $\langle n_1 n_2 | G | k_3 n_4 \rangle$ in mixed representation. Two reaction matrix elements in the laboratory frame are plotted as a function of the particle momentum k_3. The matrix element in the lower figure is dominated by the central component of the N-N interaction, while the upper one contains mostly tensor contributions.

These results are, of course, an expression of the fact that the MDFPΔ2 potential contains a much weaker tensor force and correspondingly larger central components than the RSC interaction. Its consequences are of crucial importance in the calculation of G^T_{3p1h}. While there is no intermediate state convergence problem in G^T_{3p1h} from the central-component G matrices which tend to zero already for relatively small values of k, the contribution to G^T_{3p1h} from the tensor components depends sensitively on the magnitude of $G(k)$ for large momenta k. The core polarization processes with high momentum intermediate particles are repulsive and in the case of the Reid potential, have led to converged G^T_{3p1h} results which are markedly different from the conventional $2\hbar\omega$ calculations.

We have calculated the core polarization diagram G^T_{3p1h} for several compound spectra as indicated in Fig. 1(c). Let us concentrate here on the comparison of diagrams containing $2\hbar\omega$ excitations alone with those calculated from additional plane wave intermediate particle states above the pf shell. The latter choice is regarded to be physically most appropriate.

The results for the diagonal G^T_{3p1h} matrix elements with its valence nucleons coupled to $J=0$, $T=1$ are shown in Table I. The Bonn-Jülich po-

TABLE I. Diagonal matrix elements of G_{3p1h}. The following notation for the harmonic oscillator orbitals is used: $4=0d_{5/2}$, $5=0d_{3/2}$, $6=1s_{1/2}$. Further details are given in Sec. IV.

$J=0$, $T=1$	$\langle ab \mid G_{3p1h} \mid cd \rangle$		$2\hbar\omega$	$k>10$
	44	44	−1.039 [a]	0.476
			−1.575 [b]	0.107
	55	55	−0.304 [a]	0.477
			−0.770 [b]	0.183
	66	66	+0.135 [a]	0.515
			−0.464 [b]	0.171

[a] Reid soft core.
[b] Bonn-Jülich potential.

tential leads to much more attraction for the $2\hbar\omega$ contributions to G^{T}_{3p1h} as compared with RSC. In addition, a most important result emerges from the contributions of the orthogonalized plane wave particle states beyond the pf shell ($k > 10$). While they provide a substantial repulsion in the case of the Reid potential, this same repulsion is reduced by a factor of 4 when using the Bonn-Jülich potential. We therefore can make the important statement that the Vary-Sauer-Wong effect is of negligible importance if we work with a modern meson exchange potential having a weaker tensor force. Core polarization processes can then be calculated in an excellent approximation using $2\hbar\omega$ particle-hole excitations alone. The core polarization diagram seems to be again able to provide the quadrupole-quadrupole component, the P_2 force, of the empirical effective interaction, as had been suggested long ago by Kuo and Brown.[3]

A comprehensive presentation of our results for the Vary-Sauer-Wong effect is given in Figs. 4 and 5. In Fig. 4 we compare the ^{18}O spectra which have been calculated by VSW for the Reid soft-core interaction with the spectra that we have obtained from the Bonn-Jülich potential. In Fig. 5 we present the respective results for ^{18}F. The spectra denoted by I and I′ are calculated with only $2\hbar\omega$ particle-hole excitations. II and II′ are evaluated with converged values for G_{3p1h}; i.e., p-h excitations up to $22\hbar\omega$ are included in II, while we have summed over all plane wave intermediate particle states in II′. Notice the large shifts in the calculation of Vary, Sauer, and Wong. In our calculation the discrepancy between I′ and II′ becomes much smaller. The spectra calculated from core polarization diagrams with and without high momentum intermediate particles are almost identical when using the Bonn-Jülich potential. This is another way of stating that for modern N-N interactions the so-called Vary-Sauer-Wong effect is negligible.

We now turn to the comparison of our spectra for $A = 18$ nuclei with experiment. For that purpose we calculate the effective interaction V_{eff} by evaluating the folded diagram series as des-

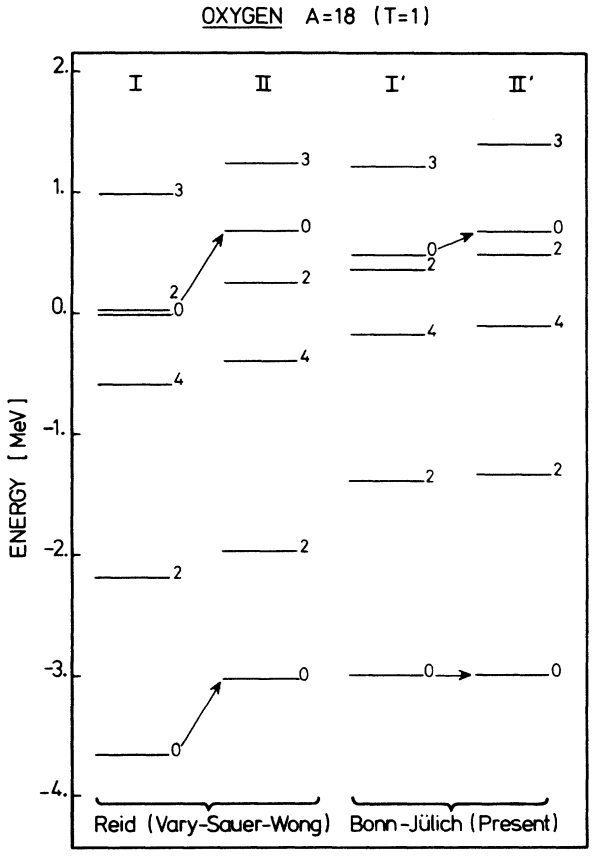

FIG. 4. Spectrum of ^{18}O ($T = 1$). No folded diagrams have been included in the calculation of the effective interaction.

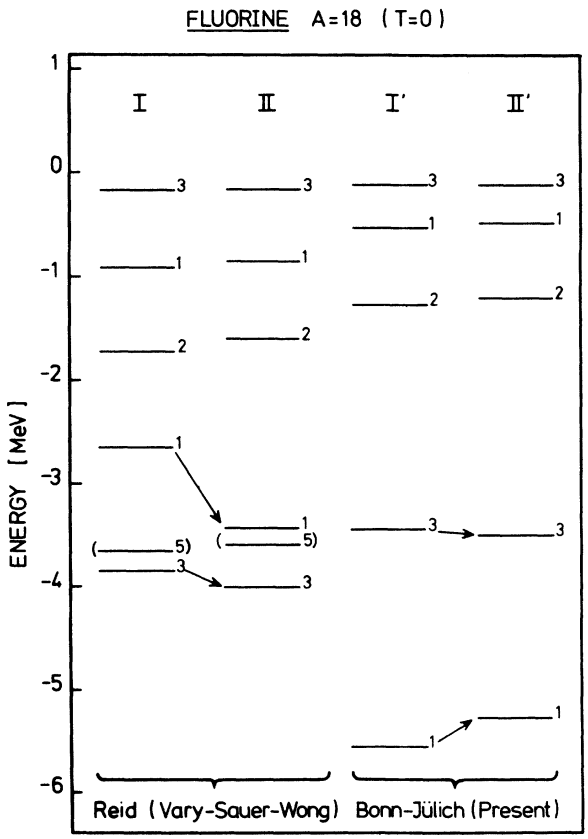

FIG. 5. Spectrum of ^{18}F ($T = 0$). No folded diagrams have been included, just as in Fig. 4.

cribed in Secs. II and III. Using the derivative method we follow closely the procedure of Shurpin *et al.*[22,23] It is then of interest to study the convergence behavior of this series as a function of the number of folds [see Fig. 1(b)]. An important feature which we have learned from our calculation is the rather sensitive dependence of the rate of convergence on the choice of the single particle spectrum. Strictly speaking, V_{eff} is independent of the single particle Hamiltonian H_0 as long as the folded diagram expansion converges. But, since we evaluate only terms with up to four folds, the result may, in fact, depend on our choice of H_0. In order to determine this dependence we have employed harmonic oscillator spectra ($\hbar\omega = 14$ MeV) with various constant shifts. According to the different shifts, we have changed the single particle energies in the *sd* shell between −5 and −13 MeV. In Table II we show the results for two matrix elements of the effective interaction, calculated from the Bonn-Jülich potential. Terms with certain numbers of folds indeed vary significantly with changes in the single particle spectrum. For example, the once-folded term for the $J=0$, $T=1$ case changes from 1.80 to 1.35 MeV when the *sd*-shell energy is shifted from −6 to −8 MeV. The corresponding change in the total V_{eff}, however, is only 0.08 MeV. We find optimal convergence behavior for *sd*-shell energies around −8 MeV. It is extremely nice to see that convergence of the folded diagram series can be obtained and that, moreover, the resulting effective interaction is rather insensitive to the choice of H_0. Tam *et al.*[21] have shown that the folded diagram series calculated with Brueckner-Hartree-Fock self-consistent spectra exhibits the same good convergence and leads to almost identical results. The folded diagrams introduce a remarkable self-correcting behavior and stability of V_{eff}. The above observations are equally true in calculations with the Reid soft-core interaction.

The $A=18$ spectra, including the contributions from high momentum particle states in G^T_{3p1h} as well as the folded diagrams, are displayed in Figs. 6 and 7 for ^{18}O and ^{18}F, respectively.

We notice the similarity of the spectra of ^{18}O derived from the meson exchange MDFPΔ2 potential and the phenomenological Reid soft-core interactions. Nevertheless, even though both theoretical ^{18}O spectra exhibit surprisingly good relative consistency, their respective 0^+ ground states are still underbound by about 1 MeV. We have seen in the case of the Bonn-Jülich potential that little repulsion comes from G^T_{3p1h} terms with particle-hole excitation energies larger than $2\hbar\omega$, resulting in a net attractive shift of roughly 800 keV with respect to the corresponding Reid G^T_{3p1h} contributions. But at the same time, the $T=1$ bare reaction matrix elements of the Bonn-Jülich potential are reduced by the quenching of the isobar terms in the potential as discussed in Sec. III. The overall situation, therefore, has not changed much and both calculations show the need of a better many-body treatment in order to explain the experimental levels.

In the case of ^{18}F the Reid soft-core potential again underbinds the low-lying levels. Historically, large deformed admixtures to the 1^+ ground

TABLE II. The convergence behavior of matrix elements of $V_{\rm eff}$ with respect to the choice of the single particle spectrum. ϵ_{sd} denotes the s-d shell single particle energy of our harmonic oscillator spectrum. See Sec. IV for further explanation.

	$\langle 0d_{5/2}0d_{5/2}\|V_{\rm eff}\|0d_{3/2}0d_{3/2}\rangle$; $J=0$, $T=1$ for the Bonn-Jülich potential					
ϵ_{sd}	Q	$-Q\int Q$	$Q\int Q\int Q$	$-Q\int Q\int Q\int Q$	$Q\int Q\int Q\int Q\int Q$	$V_{\rm eff}$(sum)
−5	−4.48	2.04	−0.85	0.48	−0.46	−3.26
−6	−4.43	1.80	−0.44	0.11	−0.13	−3.09
−7	−4.39	1.57	−0.09	−0.10	−0.02	−3.03
−8	−4.35	1.35	0.20	−0.18	−0.04	−3.01
−10	−4.26	0.94	0.62	−0.04	−0.16	−2.90
−13	−4.13	0.39	0.93	0.59	0.07	−2.17
	$\langle 0d_{5/2}0d_{3/2}\|V_{\rm eff}\|0d_{5/2}0d_{3/2}\rangle$; $J=1$, $T=0$ for the Bonn-Jülich potential					
ϵ_{sd}	Q	$-Q\int Q$	$Q\int Q\int Q$	$-Q\int Q\int Q\int Q$	$Q\int Q\int Q\int Q\int Q$	$V_{\rm eff}$(sum)
−5	−8.68	5.33	−3.96	3.84	−4.58	−8.06
−6	−8.56	4.75	−2.75	2.09	−2.15	−6.63
−7	−8.46	4.20	−1.70	0.86	−0.78	−5.87
−8	−8.35	3.67	−0.80	0.06	−0.13	−5.54
−10	−8.14	2.70	0.60	−0.52	−0.06	−5.42
−13	−7.84	1.40	1.86	0.26	−0.54	−4.86

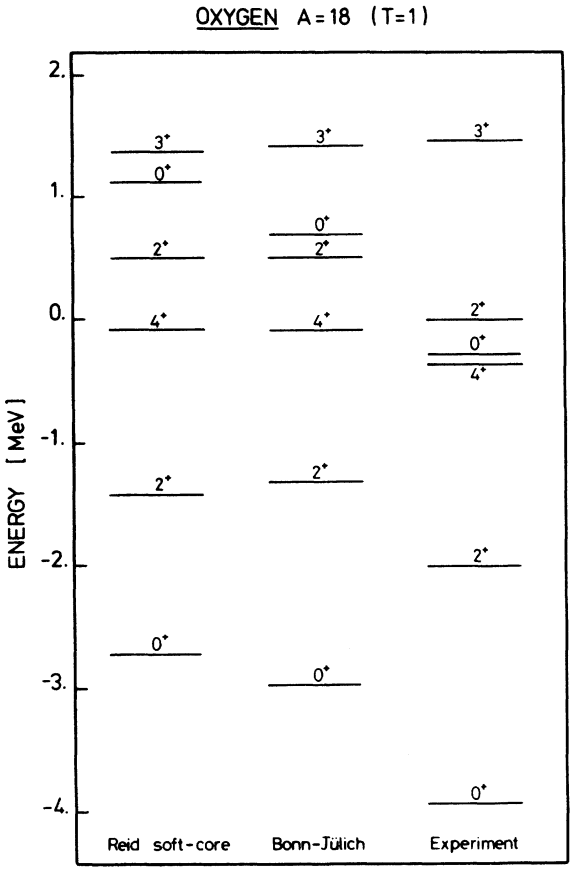

FIG. 6. Spectrum of ^{18}O ($T=1$). This spectrum was calculated with the inclusion of the folded diagrams as well as the contribution from G^{T}_{3p1h} with high momentum intermediate particle states.

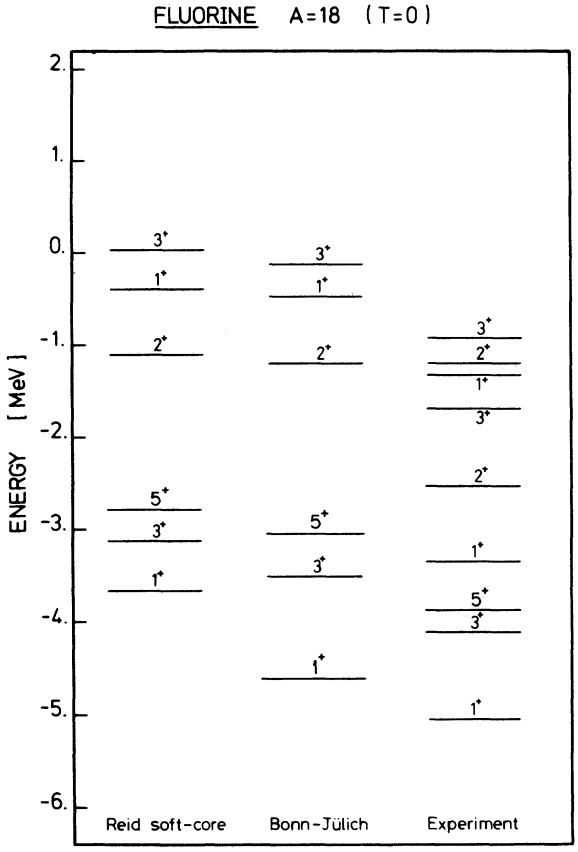

FIG. 7. Spectrum of ^{18}F ($T=0$). See explanation of Fig. 6.

state had to be invoked to explain the discrepancy between experiment and perturbation theory. As we can see in Fig. 7, however, this lowest 1^+ level received, compared with RSC, a large downward shift of about 1.0 MeV when we employed the MDFPΔ2 potential. This surprisingly larger attractiveness of the Bonn-Jülich potential in the $T=0$ channel, as compared with the Reid soft-core interaction, can be explained as follows. Both N-N interactions exhibit practically the same behavior in free space. When acting in a nuclear medium their tensor components like $\langle {}^3S_1 | V | {}^3D_1 \rangle$ $(Q/e)\langle {}^3D_1 | V | {}^3S_1 \rangle$, which are dominant for $T=0$, are reduced due to the presence of the Pauli exclusion operator. The Bonn-Jülich potential, however, contains a much smaller tensor force to begin with and consequently loses less of its strength. This results in a more attractive nuclear reaction matrix. For both ^{18}O and ^{18}F the meson exchange Bonn-Jülich potential leads to theoretical spectra which are in better agreement with experiment than the phenomenological Reid soft-core interaction.

In summary, we have shown that for a modern meson exchange interaction of the Bonn-Jülich group (MDFPΔ2) the Vary-Sauer-Wong effect is of negligible importance. This has the important consequence that core polarization processes can be calculated in a good approximation by using $2\hbar\omega$ particle-hole excitations alone. This opens up the possibility of calculating in a reliable and expedient way higher order processes. Employing the folded diagram theory convergence for the effective interaction expansion in terms of the order of folding can be obtained if an appropriate single particle spectrum is used. While the Bonn-Jülich potential provides almost sufficient attraction for

TABLE III. Matrix elements of the effective interaction as derived from the Reid soft-core potential. Detailed explanations are given in the Appendix.

TJ	$abcd$	$\langle abJT \mid V_{\text{eff}} \mid cdJT \rangle$	TJ	$abcd$	$\langle abJT \mid V_{\text{eff}} \mid cdJT \rangle$
01	4444	−0.9428	03	5555	−1.8413
01	4445	2.5485	04	4545	−3.1864
01	4455	0.8749	05	4444	−2.7687
01	4456	0.2012	10	4444	−1.6489
01	4466	−0.4938	10	4455	−3.1541
01	4544	2.4597	10	4466	−0.9163
01	4545	−4.7293	10	5544	−2.8665
01	4555	0.3870	10	5555	−0.3763
01	4556	2.0179	10	5566	−0.6681
01	4566	1.4940	10	6644	−0.8513
01	5544	0.9889	10	6655	−0.7112
01	5545	0.3343	10	6666	−0.9664
01	5555	−0.2448	11	4545	−0.0601
01	5556	−0.7448	11	4556	0.1539
01	5566	−0.2184	11	5645	0.1457
01	5644	0.1354	11	5656	0.4900
01	5645	1.9809	12	4444	−0.6207
01	5655	−0.7390	12	4445	−0.2464
01	5656	−2.9651	12	4446	−0.7456
01	5666	−0.8258	12	4455	−0.9417
01	6644	−0.4642	12	4456	0.8159
01	6645	1.4457	12	4544	−0.2706
01	6655	−0.1157	12	4545	0.0283
01	6656	−0.8859	12	4546	−0.0627
01	6666	−2.2023	12	4555	−0.7727
02	4545	−3.6993	12	4556	0.6784
02	4546	−1.1745	12	4644	−0.7326
02	4556	−1.1111	12	4645	−0.0739
02	4645	−1.1837	12	4646	−0.8839
02	4646	−0.4453	12	4655	−0.4293
02	4656	−1.9956	12	4656	1.1647
02	5645	−1.0988	12	5544	−0.7773
02	5646	−1.9456	12	5545	−0.7119
02	5656	−1.1847	12	5546	−0.4540
03	4444	−0.6847	12	5555	0.3551
03	4445	1.4474	12	5556	0.2479
03	4446	−1.3565	12	5644	0.7219
03	4455	0.4658	12	5645	0.6456
03	4544	1.3526	12	5646	1.1474
03	4545	−0.8020	12	5655	0.2700
03	4546	0.8486	12	5656	0.0875
03	4555	1.7530	13	4545	0.2022
03	4644	−1.3123	13	4546	−0.0806
03	4645	0.8469	13	4645	−0.0817
03	4646	−2.9346	13	4646	0.4429
03	4655	0.2644	14	4444	0.1491
03	5544	0.3700	14	4445	−1.1536
03	5545	1.6544	14	4544	−1.1014
03	5546	0.2619	14	4545	−0.8725

the ground state of ^{18}F, still more attraction is needed in the case of ^{18}O. It may be necessary to include core deformed states and higher order processes in order to obtain the experimental spectra. However, overall the Bonn-Jülich potential is more successful than the Reid soft-core interaction in reproducing the experimental $A = 18$ levels.

TABLE IV. Matrix elements of the effective interaction as derived from the meson exchange Bonn-Jülich potential. Detailed explanations are given in the Appendix.

TJ	$abcd$	$\langle abJT \mid V_{\text{eff}} \mid cdJT \rangle$	TJ	$abcd$	$\langle abJT \mid V_{\text{eff}} \mid cdJT \rangle$
01	4444	−1.3513	03	5555	−2.1679
01	4445	2.8204	04	4545	−3.4190
01	4455	1.3951	05	4444	−3.0342
01	4456	0.4236	10	4444	−1.8819
01	4466	−0.8164	10	4455	−3.1784
01	4544	2.7246	10	4466	−0.8879
01	4545	−5.2713	10	5544	−2.8712
01	4555	0.0923	10	5555	−0.6995
01	4556	1.6269	10	5566	−0.6240
01	4566	1.6559	10	6644	−0.8207
01	5544	1.4246	10	6655	−0.6507
01	5545	0.0486	10	6666	−1.3200
01	5555	−0.6844	11	4545	0.2345
01	5556	−0.8270	11	4556	−0.0491
01	5566	0.0852	11	5645	−0.0516
01	5644	0.3537	11	5656	0.7137
01	5645	1.5991	12	4444	−0.4825
01	5655	−0.8024	12	4445	−0.2810
01	5656	−3.0076	12	4446	−0.7123
01	5666	−0.5222	12	4455	−0.9925
01	6644	−0.8005	12	4456	0.7916
01	6645	1.6139	12	4544	−0.3024
01	6655	0.1508	12	4545	0.0994
01	6656	−0.5755	12	4546	−0.1829
01	6666	−2.5338	12	4555	−0.8360
02	4545	−3.4732	12	4556	0.6153
02	4546	−1.0983	12	4644	−0.6921
02	4556	−1.1548	12	4645	−0.1942
02	4645	−1.0973	12	4646	−0.7608
02	4646	−0.4492	12	4655	−0.5025
02	4656	−2.0468	12	4656	1.1472
02	5645	−1.1375	12	5544	−0.8476
02	5646	−1.9904	12	5545	−0.7771
02	5656	−1.1167	12	5546	−0.5076
03	4444	−0.8179	12	5555	0.4384
03	4445	1.5905	12	5556	0.2280
03	4446	−1.4043	12	5644	0.7080
03	4455	0.7839	12	5645	0.5856
03	4544	1.4978	12	5646	1.1229
03	4545	−0.8359	12	5655	0.2457
03	4546	0.8738	12	5656	0.0533
03	4555	1.7446	13	4545	0.4295
03	4644	−1.3516	13	4546	−0.0981
03	4645	0.8569	13	4645	−0.1003
03	4646	−3.0314	13	4646	0.5888
03	4655	0.2780	14	4444	0.3159
03	5544	0.6847	14	4445	−1.2618
03	5545	1.6727	14	4544	−1.1983
03	5546	0.2752	14	4545	−0.9951

ACKNOWLEDGMENTS

The authors would like to thank Dr. J. Shurpin for making available part of the computer codes and Prof. K. F. Ratcliff for many stimulating discussions. This work has been supported by the Deutsche Forschungs Gemeinschaft (DFG), through the U. S. DOE under Contract No. EY-76-S-02-3001, and by an award to one of the authors (T.T.S.K.) from the Alexander von Humboldt Foundation.

APPENDIX

The matrix elements of the effective interactions for $A = 18$ nuclei are given as derived from the

Reid soft-core potential (Table III) and the meson exchange Bonn-Jülich potential (Table IV). In this calculation we have considered the processes of Fig. 1(a) with the inclusion of high momentum intermediate states plus the effects of the folded diagrams. The matrix elements in the particle-particle coupling scheme are characterized by the total isospin T, total angular momentum J, and the single particle orbits a, b, c, and d. Our convention for the harmonic oscillator orbitals is $4 = 0d_{5/2}, 5 = 0d_{3/2}, 6 = 1s_{1/2}$.

---

*On leave from the State University of New York at Albany.

†On leave from the State University of New York at Stony Brook.

[1]G. F. Bertsch, Nucl. Phys. 74, 234 (1965).

[2]T. T. S. Kuo and G. E. Brown, Nucl. Phys. 85, 40 (1966).

[3]G. E. Brown and T. T. S. Kuo, Nucl. Phys. A92, 481 (1967).

[4]J. P. Vary, P. D. Sauer, and C. W. Wong, Phys. Rev. C 7, 1776 (1973).

[5]C. L. Kung, T. T. S. Kuo, and K. F. Ratcliff, Phys. Rev. C 19, 1063 (1979).

[6]R. V. Reid, Ann. Phys. (N.Y.) 50, 411 (1968).

[7]G. Höhler and E. Pietarinen, Nucl. Phys. B95, 210 (1975).

[8]J. W. Durso, A. D. Jackson, and B. J. Verwest, Nucl. Phys. A252, 404 (1977).

[9]H. Arenhövel and W. Fabian, Nucl. Phys. A282, 397 (1977); E. L. Lomon, Phys. Lett. 68B, 419 (1977).

[10]K. Holinde, R. Machleidt, A. Faessler, and H. Müther, Phys. Rev. C 15, 1432 (1977).

[11]K. Holinde, R. Machleidt, M. R. Anastasio, A. Faessler, and H. Müther, Phys. Rev. C 18, 870 (1978); M. R. Anastasio, A. Faessler, H. Müther, K. Holinde, and R. Machleidt, *ibid.* 18, 2416 (1978).

[12]C. W. Wong, Nucl. Phys. A91, 399 (1967).

[13]M. Baranger, in *Nuclear Structure and Nuclear Reactions*, Proceedings of the International School of Physics "Enrico Fermi," Course XI, edited by M. Jean and R. A. Ricci (Academic, New York, 1969), p. 511.

[14]T. T. S. Kuo, S. Y. Lee, and K. F. Ratcliff, Nucl. Phys. A176, 65 (1971); T. T. S. Kuo, Annu. Rev. Nucl. Sci. 24, 101 (1974).

[15]E. M. Krenciglowa and T. T. S. Kuo, Nucl. Phys. A235, 171 (1974).

[16]E. M. Krenciglowa, C. L. Kung, T. T. S. Kuo, and E. Osnes, Ann. Phys. (N.Y.) 101, No. 1, 154 (1976).

[17]C. W. Wong and D. M. Clement, Nucl. Phys. A183, 210 (1972).

[18]R. Balian and E. Brezin, Nuovo Cimento 61B, 403 (1969).

[19]S. F. Tsai and T. T. S. Kuo, Phys. Lett. 39B, 427 (1972).

[20]T. T. S. Kuo, J. Shurpin, K. C. Tam, E. Osnes, and P. J. Ellis, State University of New York at Stony Brook report (unpublished).

[21]K. C. Tam, H. Müther, M. Sommermann, T. T. S. Kuo, and A. Faessler, University of Tübingen report (unpublished).

[22]J. Shurpin, D. Strottmann, T. T. S. Kuo, M. Conze, and P. Manakos, Phys. Lett. B69, 395 (1977).

[23]J. Shurpin, H. Müther, T. T. S. Kuo, and A. Faessler, Nucl. Phys. A293, 61 (1977).